

Dual-parameter sensing characteristics of a single fiber Bragg grating half-pasted by 1C-LV epoxy under different curing

HONG LI^{1,3}, HAoyue ZHANG¹, YANMING SONG³, FANYONG MENG¹, LIANQING ZHU^{1,2*}

¹Key Laboratory of the Ministry of Education for Optoelectronic Measurement Technology and Instrument, Beijing Information Science & Technology University, Beijing, 100016, People's Republic of China

²Overseas Expertise Introduction Center for Discipline Innovation ("111 Center"), Beijing Information Science & Technology University, Beijing, 100192, People's Republic of China

³Beijing Laboratory of Optical Fiber Sensing and System, Beijing Information Science & Technology University, Beijing, 100016, People's Republic of China

*Corresponding author: zlj_jxq@sina.com

A novel technology for the simultaneous and independent measurement of dual parameters is proposed and experimented. By using a single fiber Bragg grating half-pasted by 1C-LV epoxy under different curing conditions, the sensor structure is designed such that the reflective single-peak spectrum splits into a twin-peak spectrum, which makes the FBG spectrum form a natural spectral peak splitting bias. A measurement limitation exists in the FBG sensor packaging at room temperature, which can be solved by the high-temperature cured packaging method. To verify the validity of the theory and methodology, the experimental system is used. In the range from -1000 to $+1000$ $\mu\epsilon$ and from 35 to 75°C , the Bragg wavelength change is relative linear to the strain and temperature. The temperature and strain variations can be independently and simultaneously measured using the split peak, and the deviations of the FBG sensor are $\pm 1^\circ\text{C}$ and ± 5 $\mu\epsilon$, respectively. This single FBG sensor can realize dual-parameter measurement, which is valuable for narrow-space health monitoring.

Keywords: fiber Bragg grating, cross-sensitivity, double peaks, surface pasting, curing.

1. Introduction

The fiber Bragg grating (FBG) has attracted considerable attention because of its distinguished advantages when it is compared with electric sensors owing to its electromagnetic interference immunity, high sensitivity, compact size and so on [1–6]. Utilizing the characteristics feature that the Bragg wavelength of FBG shifts owing to the effect of

temperature and strain, many types of FBG-based sensors have been manufactured [7]. However, one of the most significant limitations of the Bragg gratings is their intrinsic temperature cross-sensitivity, superimposed on the strain effects [8–11]. When the temperature and strain change together, the shift of the single FBG Bragg wavelength cannot distinguish them. For the 1.55 μm FBG, the wavelength shifts in unit temperature and unit strain are approximately 10.8 pm/ $^{\circ}\text{C}$ and 1.2 pm/ $\mu\epsilon$, respectively [12]. The 1 $^{\circ}\text{C}$ shifts of temperature will result in about 10 $\mu\epsilon$ strain measurement error. Therefore, temperature compensation is necessary for strain measurement, particularly for long-term structural health monitoring using FBG sensors.

To realize the practical applications of FBG sensors, discrimination techniques must be discovered to reveal individual parameters, in which the cross-sensitivity between temperature and strain is one of the most fundamental issues. Several techniques have been proposed for the discrimination of the strain and thermal effects, such as the reference-grating technique, dual-wavelength technique [11], and dual-parameter simultaneous measurement technique, writing two FBGs in a different diameter fiber, combining FBG with a Fabry–Pérot cavity, FBG with some micro-channel, and the strain-free FBG compensation method [11, 13–19]. The reference-grating technique requires at least two FBGs, which take up more space on the test surface and also lead to increased demodulation data. The dual-wavelength method requires a large difference in FBG wavelength or a different wavelength band source. In the dual-parameter method, the sensitivity coefficients of the two FBGs are very close, which leads to morbid equations and cause large calculation errors. A half-encapsulated FBG sensor is easy to fabricate, and can reduce the complexity and cost of the system. PARNE SAIDI REDDY *et al.* [20] proposed a simple sensor using half the length of a 3-cm fiber Bragg grating embedded on a cantilever for the simultaneous measurement and discrimination of strain and temperature. When the strain is increased, the shift also increases accordingly; thereby, the reflected spectrum from the sensor shows two peaks, one remains constant, whereas the other shifts according to the applied strain. However, in this way, spectral division is not obvious in the range of small strain changes, and it is difficult to obtain the two peaks at this time. Spectrum distortion, which may be induced by overlapping or non-uniform strains, may hinder the adoption of this technique. In order to this issue, WANG *et al.* [21] adopted an improved particle swarm optimization based spectra reconstructing method to estimate the temperature and mean strain according to the distorted spectrum, which was to try to address the distorted spectra of the two split peaks.

In this paper, a dual-parameter sensing method based on a novel surface pasting technology has been proposed, which is based on a single FBG sensor half-pasted by 1C-LV epoxy under different curing conditions. FBG with high temperature curing and semi-adhesive appeared split front first, forming a natural peak bias. The exposed part of the Bragg grating is used to measure temperature changes, and the cured part is used to measure temperature and strain changes. We screened and verified the type of glue and the curing temperature in advance. The theoretical analysis and experimental measurement are carried out to study the dual-parameter sensing characteristics.

2. FBG sensing principle

Fiber Bragg grating is a passive optical component written in the fiber. The phase mask and ultraviolet (UV) laser exposure are used to write the fiber grating as shown in Fig. 1. Ultraviolet light normal to the phase mask passes through and is diffracted by the periodic corrugations of the phase mask. The two diffracted ± 1 order beams interfere with each other to produce a periodic pattern that photo-imprints a corresponding grating in the optical fiber. FBG consists of periodic refractive index modulation in the core of a single-mode optical fiber. The refractive index of the fiber is periodically distributed due to the UV radiation, and the spectrum signal is periodically modulated. It behaves as a wavelength selective filter that reflects light signals at a specific wavelength called the Bragg wavelength λ_B . Based on the coupled mode theory, the reflection wavelength of a periodic FBG is defined by the relationship [22, 23]

$$\lambda_B = 2n_{\text{eff}}\Lambda \quad (1)$$

where n_{eff} is the effective refractive index of the fiber, and Λ is the grating period. It can be noted that either the grating period change or the effective refractive index variation can lead to the FBG wavelength shift. The change of wavelength of the FBG due to strain and temperature can be approximately described by equation

$$\frac{\Delta\lambda_B}{\lambda_B} = (1 - P_e)\Delta\varepsilon + (\alpha + \zeta)\Delta T \quad (2)$$

where λ_B is the original wavelength, $\Delta\lambda_B$ is the wavelength shift, $\Delta\varepsilon$ is the change of strain experienced by the grating, and P_e is the elasto-optical coefficient. Under the room temperature, $P_e \approx 0.22$. The second expression describes the impact of temperature on the wavelength shift, where ζ is thermo-optical coefficient, α is thermo-elastic coefficient and ΔT is the temperature variation. As the spectrum responds to both strain and temperature, it needs to account for both effects and distinguish between them.

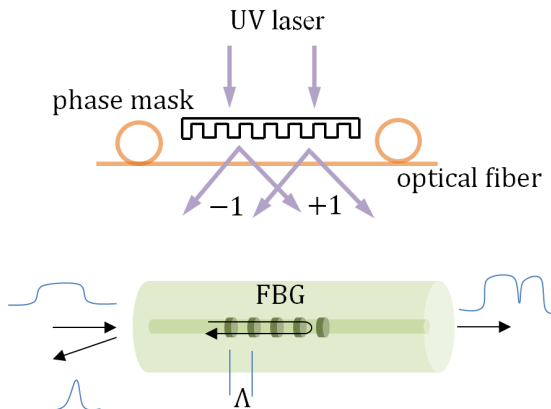


Fig. 1. Schematic diagram of FBG written and its spectral transmission characteristics.

For proper strain measurement, the temperature effects on FBG sensors must be compensated. It can be overcome by installing a FBG for temperature measurement in close thermal contact with the strain sensor. A temperature compensated strain value can yield through a simple subtraction of the wavelength shift of FBG temperature sensor from the shift of FBG strain.

3. FBG pasting method and experimental setup

3.1. Selection of FBG surface adhesive

The strain change can be measured when FBGs are attached to the surface of the substrate, so the surface adhesive is very critical. The surface adhesive layer of FBG should meet the following requirements: (1) it can stick the fiber to the substrate well and has low creep, (2) after curing, it has certain toughness and high strength, (3) good long-term stability, aging resistance, it can adapt to the harsh environment.

After comparing the parameter characteristics of various epoxy adhesives, we selected five epoxy adhesives suitable for the combination of metal structure and optical fiber. They are 3M DP-420, 353ND, M-bond 610, Loctite 1C-LV, 502. And the surface

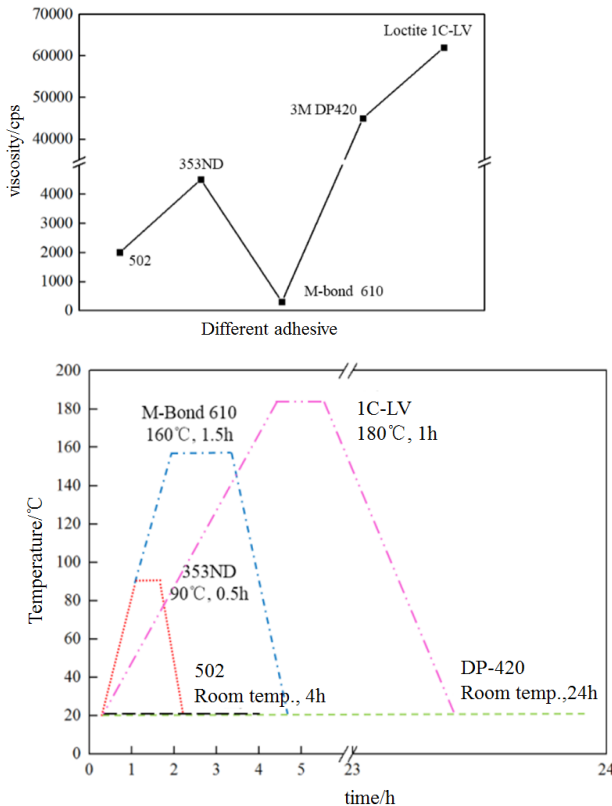


Fig. 2. Specification of different adhesives.

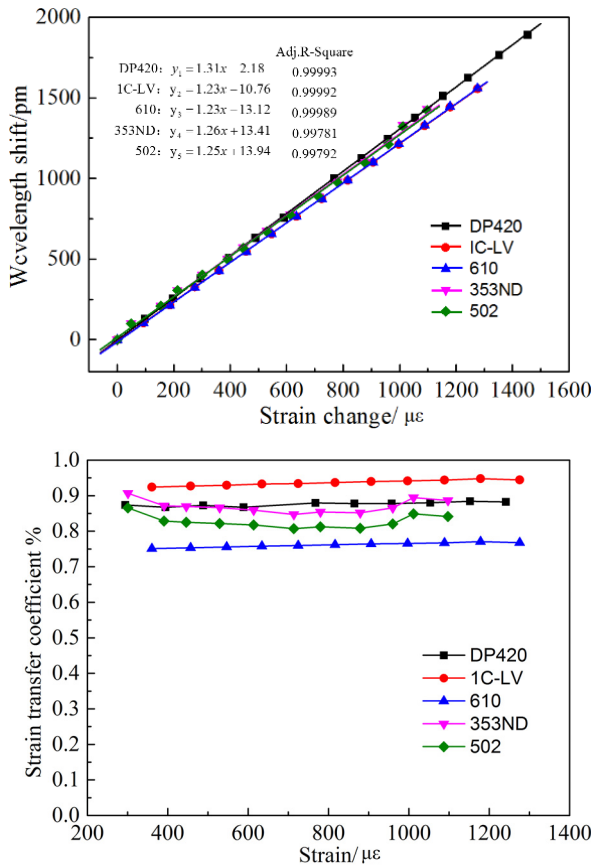


Fig. 3. FBG strain characteristics under different epoxy glue.

adhesive effect test was carried out. The viscosity and curing process characteristics of different adhesives are shown in Fig. 2.

Five similar fiber Bragg gratings were pasted on the standard tensile test piece with these five epoxy adhesives, respectively. The resistance strain bridge is pasted at the same horizontal position of the FBG and the strain value is recorded. Each set of samples is equipped with a temperature supplement FBG. Tensile force was applied to the test sample by MTS material testing machine. Figure 3 shows the strain characteristics of FBGs under different adhesive conditions. The tensile test results show a good linear relationship. The strain sensitivity coefficient varies with different adhesive types. Among them, 1C-LV has the best strain transfer coefficient.

3.2. Half-pasted under different curing

Two FBGs of 24 mm length were fabricated by a phase mask method and UV laser of 244 nm wavelength. The full width at half maximum of the FBGs is approximately 0.15 nm, and they have the central wavelength values of 1553.56 nm (FBG1) and

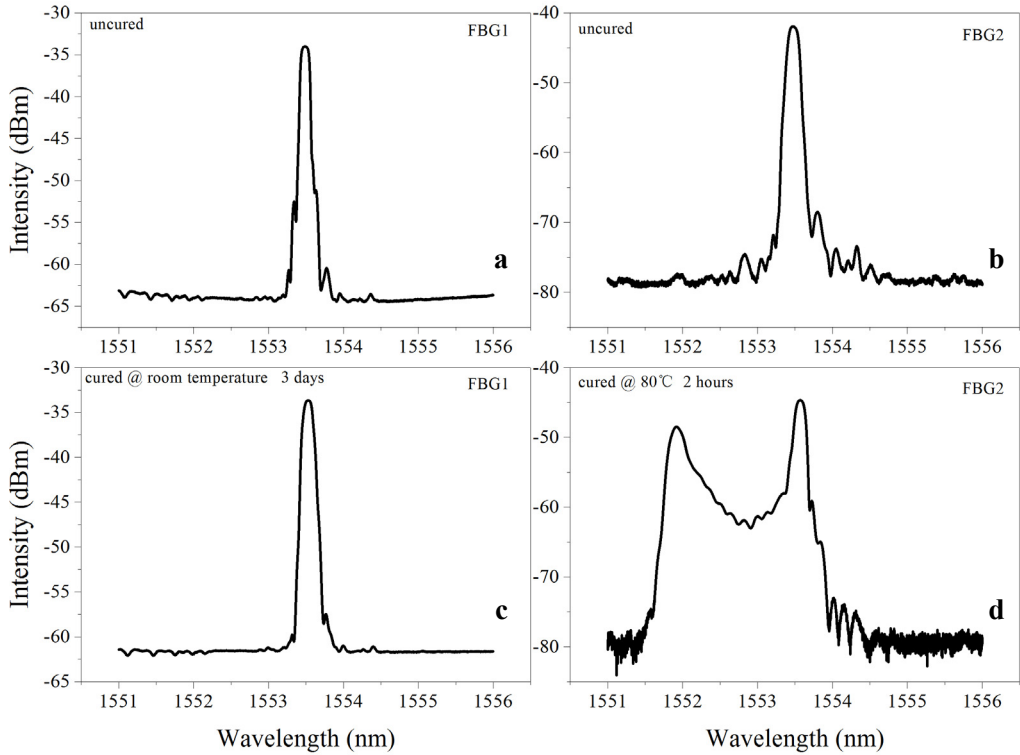


Fig. 4. Reflection spectra of FBG1 and FBG2 before and after curing. Before curing at room temperature (a), after curing at room temperature (b), before curing at 80° (c), and after curing at 80° (d).

1553.57 nm (FBG2). Figures 4a and 4b show the spectra of the FBGs before pasting. Unpackaged FBG is pasted on the equal-strength beam as shown in Figs. 5a–5c. Half of the length of the FBG is fixed to the beam with epoxy adhesive (Loctite 1C-LV). The other half of the FBG is freely stretched with a tape. 1C-LV has two curing conditions: complete curing is obtained after 3 days at room temperature (FBG1) and cur-

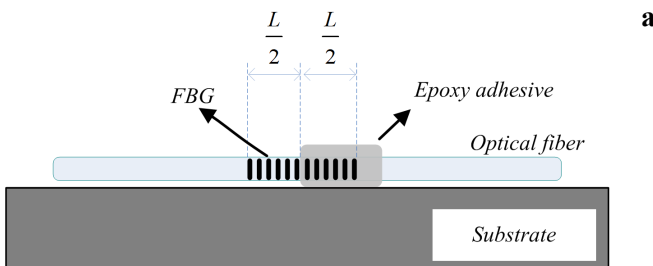


Fig. 5. FBG sensor pasted on the equal-strength beam (a), the strain experimental photograph (b), and the temperature experimental photograph (c). Photographic overviews of the experiment setup (d, e).

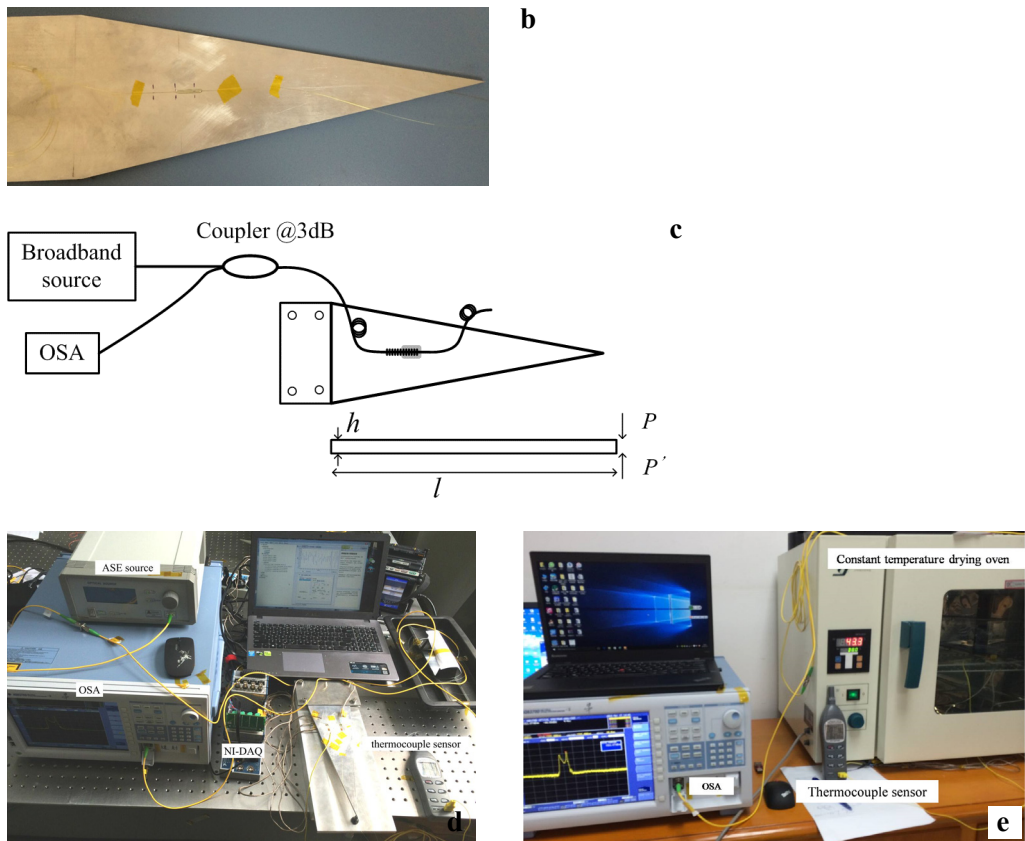


Fig. 5. Continued.

ing with heat such as for two hours at 80° is also possible (FBG2). Figures 4c and 4d show the spectra of the FBGs after pasting.

Half-length of the FBG was pasted with epoxy to the substrate, whereas the other half was in a free state. The pasted length of the FBG is sensitive to both strain and temperature variations, whereas the free length of the FBG is only sensitive to temperature variation.

The host material of the uniform-strength beam is Magnalium 7075-T6. The length and thickness of the equal-strength beam are 280 and 4 mm, respectively. One micrometer head (Newport SM-25, read directly in increments of $10\ \mu\text{m}$, and 25 mm travel range) was used to adjust the deflection of the beam end. The strain value of the equal-strength beam can be calculated by measuring the deflection, which is associated with the geometry size and unrelated with the elasticity modulus. The system is composed of an ASE source, a 3 dB fiber coupler with a 50:50 splitting ratio, a psychrometer (AZ 8746), and an optical spectrum analyzer (YOKOGAWA AQ6370D), as shown in Figs. 5d and 5e.

A uniform isosceles triangle cantilevered beam can be used as a uniform-strain agent. The axial strain ε of the beam is given by [24]

$$\varepsilon = \frac{6lF}{Ech^2} \quad (3)$$

where h , l , and c are the thickness, length, and base length of the beam, respectively. F is the force applied vertically to the free end of the cantilever, and E is the Young's modulus of the beam material. Considering Eq. (3), the relationship between the axial strain of the beam, ε , and displacement of the free end of the cantilever, d , can be expressed as

$$d = \frac{\varepsilon l^2}{h} \quad (4)$$

4. Experiment and discussion

Under the room-temperature curing conditions, the response to strain change of FBG1 is as shown in Figs. 6a–6d. When the two peaks of FBG1 split and become smaller, the demodulation devices or optical spectrum analyzer (OSA) cannot easily find the peak, with some deficiency at a small strain change range, which is the measurement limitation of the packaged FBG sensor.

However, under the high-temperature curing conditions, owing to the heat expansion and cold contraction effects, the grating period Λ' and the effective refractive index n'_{eff} of the fixed FBG2 segment changed, which caused the Bragg wavelength to change. Then, the reflected Bragg wavelength will also split into two parts, namely,

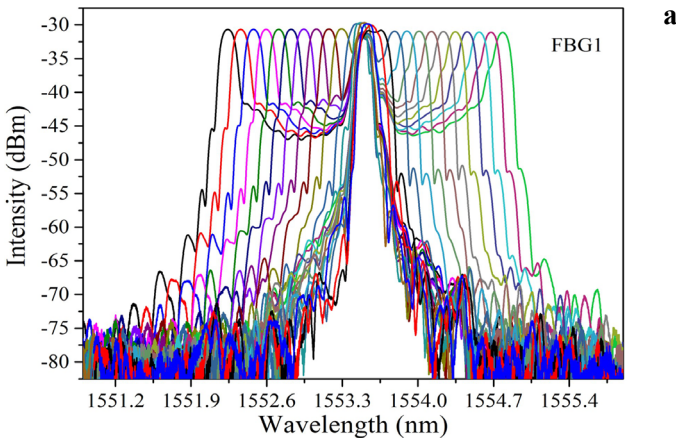
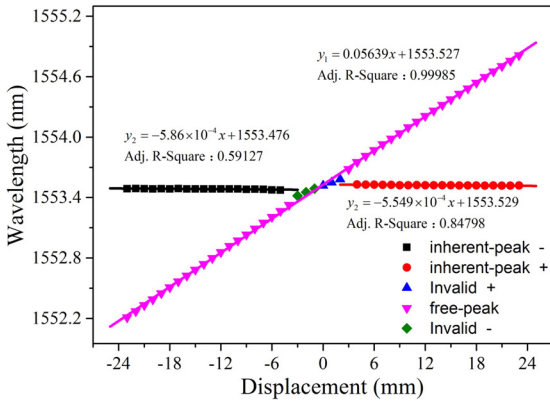
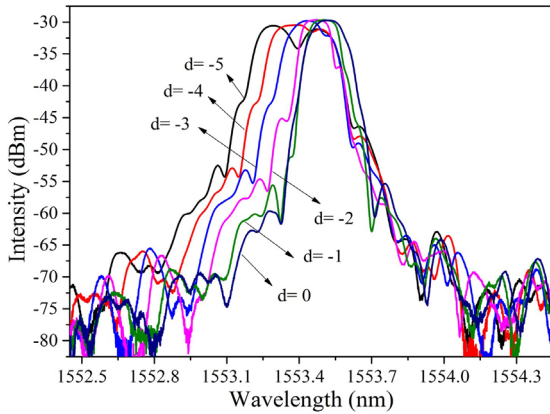


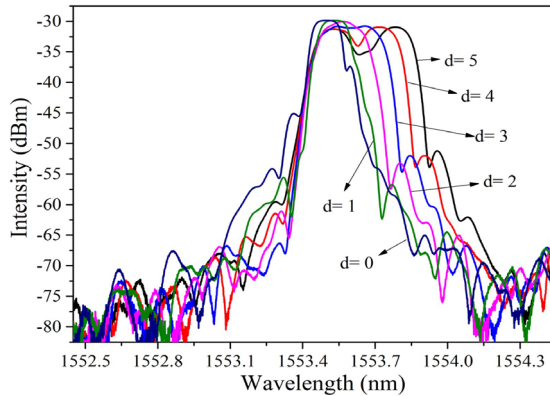
Fig. 6. Displacement experimental results of FBG cured at room temperature for 3 days. Reflection spectra for different displacements (a), and measured Bragg wavelength shifts of the sensor in response to displacement change (b). Reflection spectra for displacement change in the ranges from -5 to 0 mm (c), and from 0 to 5 mm (d).



b



c



d

Fig. 6. Continued.

λ_{B1} and λ_{B2} . Because of the high temperature curing in the half-pasted state, the original FBG spectrum appeared split and shift. The original single FBG2 actually turned into two FBGs: the inherent peak (λ_{B1}) and the free peak (λ_{B2}). Figure 7a shows the reflection spectra for different strains with a constant temperature. λ_{B1} does not shift because

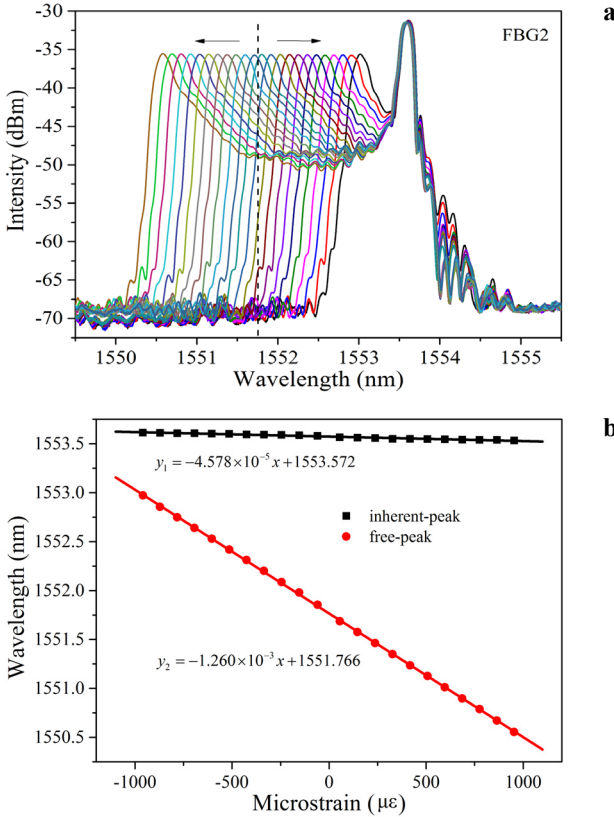


Fig. 7. Microstrain experimental results of FBG cured at 80°C for 2 h. Reflection spectra for different displacements (a), and measured Bragg wavelength shifts of the sensor in response to microstrain change (b).

of the constant temperature, whereas λ_{B2} shifts to the longer or shorter wavelength corresponding to the applied tensile or compressive strain. Figure 7b shows the wavelength changes under the different displacements. The black line is the fitted line of the inherent peak, and the red line is the fitted line of the free peak.

We maintained the beam freely under no deformation and plunged the FBG structure (including stage) into an electric heating constant-temperature drying oven (DHG-9503A); the temperature was detected with a thermocouple sensor. The measurement range was 35–75°C. Figure 8a shows the reflection spectra at three different temperatures with a constant strain. The two split wavelengths shifted to longer wavelengths at different rates, whereas the free peaks shifted faster than the inherent peaks. The experimental results are shown in Fig. 8b. Because half of FBG2 is packaged by 1C-LV under 80°C curing, the thermal effects of the substrate and epoxy adhesive actually act on the segment FBG, which revealed that the free peak shifts faster.

When the substrate varied in axial strain and temperature, the shift of λ_{B1} corresponded to the temperature variation, whereas the shift of λ_{B2} was associated with the

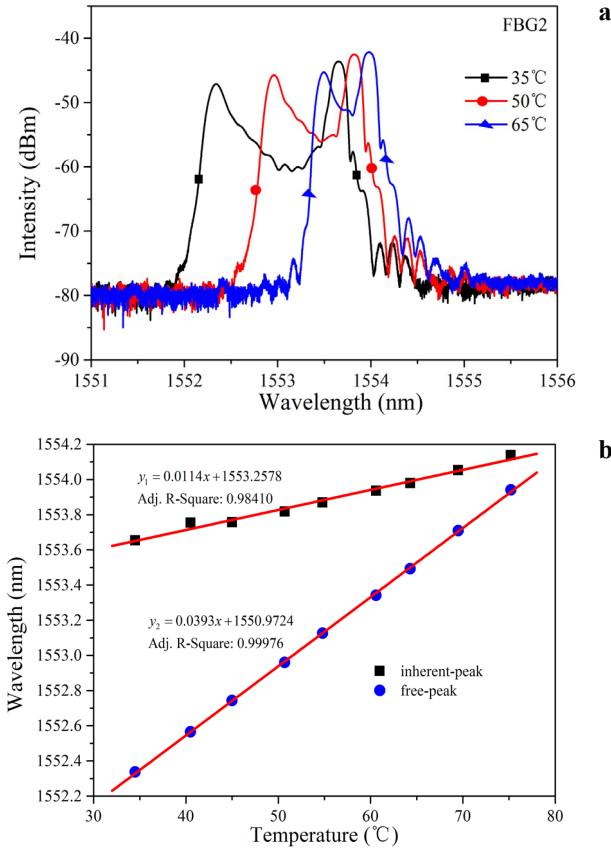


Fig. 8. Temperature experimental results. Reflection spectra for different temperatures (a), and measured Bragg wavelength shifts of the sensor in response to temperature change (b).

combined temperature and strain variations. The shifts of these two wavelengths can be expressed as [8]

$$\Delta\lambda_{B1} = \frac{\lambda'_{B1} - \lambda_{B1}}{\lambda_{B1}} = (\alpha + \zeta)\Delta T \quad (5)$$

and

$$\Delta\lambda_{B2} = \frac{\lambda'_{B2} - \lambda_{B2}}{\lambda_{B2}} = \left[(1 - P_e)\alpha_{\text{sub}} + \zeta \right] \Delta T + \lambda_{B2}(1 - P_e)\varepsilon \quad (6)$$

where λ_{B1} and λ_{B2} are the original Bragg wavelengths of the inherent peak and free peak, λ'_{B1} and λ'_{B2} are the measured wavelengths, respectively, P_e is the effective photoelastic constant (~ 0.22) of the fiber material, α is the linear expansion with the

value of $2.3 \times 10^{-6}/^{\circ}\text{C}$, ζ is the thermo-optic coefficient with a value of $7 \times 10^{-6}/^{\circ}\text{C}$, and ε is the longitudinal strain. Let α_{sub} be the thermal expansion coefficient of the substrate material. For $\alpha_{\text{sub}} \gg \alpha$ (for example, $\alpha_{\text{sub}} = 23 \times 10^{-6}/^{\circ}\text{C}$ for aluminum), the relative change in the Bragg wavelength with temperature can be given by

$$\begin{cases} \lambda'_{\text{B1}} = \lambda_{\text{B1}}(\alpha + \zeta)\Delta T + \lambda_{\text{B1}} \\ \lambda'_{\text{B2}} = \lambda_{\text{B2}}\left[(1 - P_e)\alpha_{\text{sub}} + \zeta\right]\Delta T + \lambda_{\text{B2}}(1 - P_e)\varepsilon + \lambda_{\text{B2}} \end{cases} \quad (7)$$

When the temperature was constant, λ'_{B1} did not change, and λ'_{B2} was related only to the strain. These wavelengths can be expressed as

$$\begin{cases} \lambda'_{\text{B1}} = \lambda_{\text{B1}} \\ \lambda'_{\text{B2}} = \lambda_{\text{B2}}(1 - P_e)\varepsilon + \lambda_{\text{B2}} \end{cases} \quad (8)$$

When there is no strain, they can be expressed as

$$\begin{cases} \lambda'_{\text{B1}} = \lambda_{\text{B1}}(\alpha + \zeta)(T' - T_0) + \lambda_{\text{B1}} \\ \lambda'_{\text{B2}} = \lambda_{\text{B2}}\left[(1 - P_e)\alpha_{\text{sub}} + \zeta\right](T' - T_0) + \lambda_{\text{B2}} \end{cases} \quad (9)$$

From Equations (5) and (6), it is known that by measuring the shift of the inherent-peak wavelength λ'_{B1} and the free-peak wavelength difference λ'_{B2} , the temperature variation and strain can be determined directly.

To verify the validity of the double-parameter simultaneous measurement, a strain bridge was installed in the same cross-section of the equal-strength beam. The encapsulated foil gauges used were the single-element-type KFR-1-350-C1-23(KYOWA). The adhesive used for pasting the gauges was CC-33A (KYOWA). The foil strain gauge instrumentation was composed of a commercial 4-channel simultaneous bridge module (National Instrument C series strain/bridge input module NI-9237) utilizing transducer-dependent signal conditioning electronics as needed. Data was acquired at 1 kHz and transferred to a real-time computer through a 24-bit parallel interface. Figure 9 shows the H-bridge strain gauge position. Another FBG temperature sensor was se-

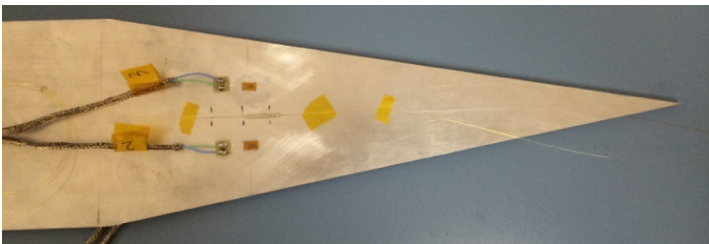


Fig. 9. Layout of the H-bridge strain gauge.

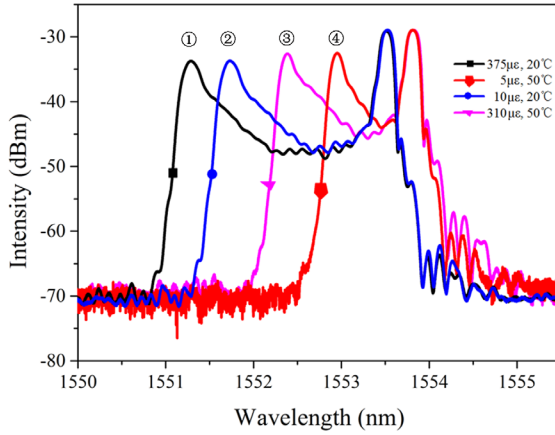


Fig. 10. Comparison of reflection spectra in different microstrains and temperatures.

lected for comparison. Under different microstrains and temperatures, the reflection spectra of the FBG sensor are as shown in Fig. 10.

According to the calculation result, the temperature and microstrain are $T = 50.7^{\circ}\text{C}$ and $\varepsilon = 323 \mu\text{ε}$, respectively. The temperature measured by the thermocouple sensor is 50.1°C , and the strain gauge monitoring result is $319.6 \mu\text{ε}$. Figure 11 shows the temperature and microstrain deviations calculated according to six groups of sampling data of the FBG sensor, which are $\pm 1^{\circ}\text{C}$ and $\pm 5 \mu\text{ε}$, respectively.

According to the analysis of results in Figs. 7a, 8a and 10, it can be seen that the measurement range of the manufactured sensor is related to the splitting peak offset amount after FBG half-pasted curing. One of the splitting peaks is only sensitive to temperature, while the other can reflect strain and temperature, so theoretically the change of the peak distance between the two splitting peaks is the strain value. However, due to the thermal transfer of epoxy glue and the thermal effect of epoxy glue

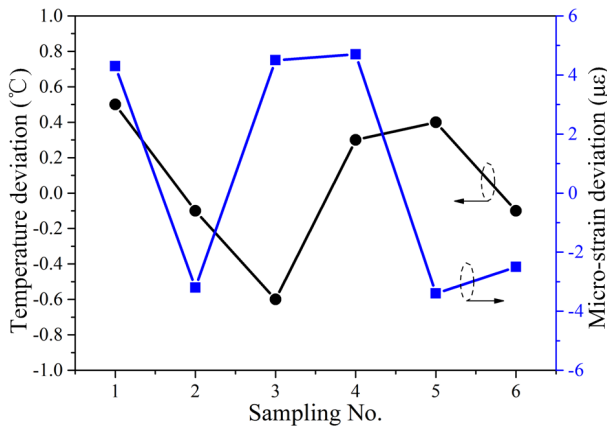


Fig. 11. Dual-parameter measurement deviations.

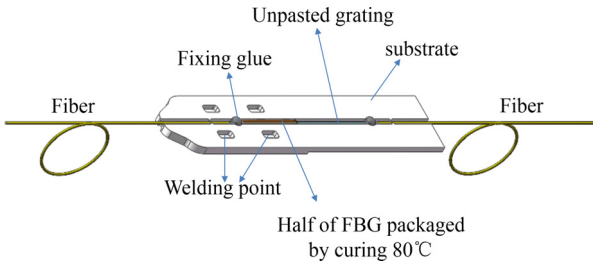


Fig. 12. Sensor packaging structure.

itself, it is still necessary to establish a set of equations with free peak to calculate the temperature and strain double parameters according to the calibrated temperature sensitivity coefficient and strain sensitivity coefficient, so as to ensure the measurement value is more accurate.

Combining Eqs. (3) and (7) shows that the wavelength difference is only sensitive to the cantilever deflection, which is induced by the placement of the free end, and the wavelength shifts of the free section of FBG are only sensitive to temperature variation. Therefore, by measuring the shift λ'_{B1} of the shorter Bragg wavelength, the temperature variation can be measured. Moreover, by detecting the wavelength difference λ'_{B2} , the displacement of the free end of the cantilever can then be measured. As the information, associated with the temperature variation and displacement, is not cross-talking, each can be measured directly and easily. The sensor packaging structure was designed on the basis of the above principle, as shown in Fig. 12.

5. Conclusions

In conclusion, a novel approach with simple FBG structures has been proposed, which employed a single half-pasted fiber Bragg grating cured at high temperature to measure strain and temperature independently and simultaneously, only by monitoring the wavelength of the double-peak FBG sensor. This surface pasting method makes the FBG spectrum form a natural spectral peak splitting bias, which solves the problem that the spectral division is not obvious when the small strain changes in the traditional normal temperature half paste method.

The experimental result showed that the Bragg wavelength change is linear to the strain and temperature. Thus, the thermal effect can be eliminated easily. The FBG sensor can realize dual-parameter measurement, which is suitable for narrow-space health monitoring and distributed measurement. In addition to its ability to simultaneously measure dual parameters effectively, the approach has the characteristics of simplicity and low cost.

This paper has proved the advantages of the high temperature curing half-pasted method. However, there are many kinds of FBG surface adhesives. With the development of materials, more adhesives with good performance may appear, which are suit-

able for this type of surface adhesive. In addition, the consistency and stability of the encapsulation performance of epoxy adhesive under different curing conditions need to be explored deeply.

Acknowledgment – This work was supported by the Beijing Municipal Natural Science Foundation (4194077), National Natural Science Foundation of China (61903042, 61735002), Vertical subject of Beijing laboratory (Z2018020) and Research Project of Beijing Education Committee (KM201811232006). The authors declare that they have no conflict of interest.

References

- [1] MIZUTANI Y., GROVES R.M., *Multi-functional measurement using a single FBG sensor*, Experimental Mechanics **51**, 2011, pp. 1489–1498, DOI: [10.1007/s11340-011-9467-2](https://doi.org/10.1007/s11340-011-9467-2).
- [2] SCHUKAR V., KUSCHE N., KALINKA G., HABEL W., *Field deployable fiber Bragg grating strain patch for long-term stable health monitoring applications*, Applied Sciences **3**(1), 2013, pp. 39–54, DOI: [10.3390/app3010039](https://doi.org/10.3390/app3010039).
- [3] LU L.D., ZHUANG W., LI H., LOU X., ZHU L., *Fiber Bragg grating-based measurement of random -rotation parameters*, Applied Optics **56**(2), 2017, pp. 211–217, DOI: [10.1364/AO.56.000211](https://doi.org/10.1364/AO.56.000211).
- [4] WANG G., XING F., WEI M., YOU Z., *Precision enhancement method for multiplexing image detector -based sun sensor with varying and coded apertures*, Applied Optics **54**(35), 2015, pp. 10467–10472, DOI: [10.1364/AO.54.010467](https://doi.org/10.1364/AO.54.010467).
- [5] LI H., ZHU L.Q., DONG M., LOU X., GUO Y., *Analysis on strain transfer of surface-bonding FBG on Al 7075-T6 alloy host*, Optik **127**(3), 2016, pp. 1233–1236, DOI: [10.1016/j.jilleo.2015.10.227](https://doi.org/10.1016/j.jilleo.2015.10.227).
- [6] OZOLINS O., BOBROVS V., *Theoretical study of all-optical RZ-OOK to NRZ-OOK format conversion in uniform FBG for mixed line-rate DWDM systems*, Chinese Optics Letters **13**(6), 2015, article 060603.
- [7] LIN G.C., WANG L., YANG C.C., SHIH M.C., CHUANG T.J., *Thermal performance of metal-clad fiber Bragg grating sensors*, IEEE Photonics Technology Letters **10**(3), 1998, pp. 406–408, DOI: [10.1109/68.661425](https://doi.org/10.1109/68.661425).
- [8] LI J., XING F., CHU D., LIU Z., *High-accuracy self-calibration for smart, optical orbiting payloads integrated with attitude and position determination*, Sensors **16**(8), 2016, p. 1176, DOI: [10.3390/s16081176](https://doi.org/10.3390/s16081176).
- [9] LI L.T., ZHANG D.S., WEN X., PENG S., *FFPI-FBG hybrid sensor to measure the thermal expansion and thermo-optical coefficient of a silica-based fiber at cryogenic temperatures*, Chinese Optics Letters **13**(10), 2015, article 100601.
- [10] WANG Y.X., BAO H.H., RAN Z.L., HUANG J.W., ZHANG S., *Integrated FP/RFBG sensor with a micro -channel for dual-parameter measurement under high temperature*, Applied Optics **56**(15), 2017, pp. 4250–4254, DOI: [10.1364/AO.56.004250](https://doi.org/10.1364/AO.56.004250).
- [11] XU M.G., ARCHAMBAULT J.L., REEKIE L., DAKIN J.P., *Discrimination between strain and temperature effects using dual-wavelength fibre grating sensors*, Electronics Letters **30**(13), 1994, pp. 1085–1087, DOI: [10.1049/el:19940746](https://doi.org/10.1049/el:19940746).
- [12] MOREY W.W., MELTZ G., GLENN W.H., *Fibre optic Bragg grating sensors*, Proceedings of SPIE **1169**, 1990, pp. 98–107, DOI: [10.1117/12.963022](https://doi.org/10.1117/12.963022).
- [13] KERSEY A.D., BERKOFF T.A., MOREY W.W., *Multiplexed fiber Bragg grating strain-sensor system with a fiber Fabry–Perot wavelength filter*, Optics Letters **18**(16), 1993, pp. 1370–1372, DOI: [10.1364/OL.18.001370](https://doi.org/10.1364/OL.18.001370).
- [14] DONG X.Y., LIU Y.Q., LIU Z., DONG X., *Simultaneous displacement and temperature measurement with cantilever-based fiber Bragg grating sensor*, Optics Communications **192**(3–6), 2001, pp. 213–217, DOI: [10.1016/S0030-4018\(01\)01157-9](https://doi.org/10.1016/S0030-4018(01)01157-9).

- [15] SENGUPTA D., SAI SHANKAR M., SAIDI REDDY P., SAI PRASAD R.L.N., SRIMANNARAYANA K., *Sensing of hydrostatic pressure using FBG sensor for liquid level measurement*, *Microwave and Optical Technology Letters* **54**(7), 2012, pp. 1679–1683, DOI: [10.1002/mop.26890](https://doi.org/10.1002/mop.26890).
- [16] SHEN C.Y., ZHONG C., *Novel temperature-insensitive fiber Bragg grating sensor for displacement measurement*, *Sensors and Actuators A: Physical* **170**(1–2), 2011, pp. 51–54, DOI: [10.1016/j.sna.2011.05.030](https://doi.org/10.1016/j.sna.2011.05.030).
- [17] HUANG J., ZHOU Z.D., WEN X.Y., ZHANG D.S., *A diaphragm-type fiber Bragg grating pressure sensor with temperature compensation*, *Measurement* **46**(3), 2013, pp. 1041–1046, DOI: [10.1016/j.measurement.2012.10.010](https://doi.org/10.1016/j.measurement.2012.10.010).
- [18] PEREIRA G., MCGUGAN M., MIKKELSEN L.P., *Method for independent strain and temperature measurement in polymeric tensile test specimen using embedded FBG sensors*, *Polymer Testing* **50**, 2016, pp. 125–134, DOI: [10.1016/j.polymertesting.2016.01.005](https://doi.org/10.1016/j.polymertesting.2016.01.005).
- [19] OORE S., OORE M., *Uniform strength for large deflections of cantilever beams under end point load*, *Structural and Multidisciplinary Optimization* **38**, 2009, pp. 499–510, DOI: [10.1007/s00158-008-0291-y](https://doi.org/10.1007/s00158-008-0291-y).
- [20] PARNE SAIDI REDDY, SAI PRASAD R.L.N., SEN GUPTA D., SAI SHANKAR M., SRIMANNARAYANA K., TIWARI U., MISHRA V., *A simple FBG sensor for strain–temperature discrimination*, *Microwave and Optical Technology Letters* **53**(5), 2011, pp. 1021–1024, DOI: [10.1002/mop.25901](https://doi.org/10.1002/mop.25901).
- [21] WANG Z.F., WANG J., SUI Q.M., JIA L., *The simultaneous measurement of temperature and mean strain based on the distorted spectra of half-encapsulated fiber Bragg gratings using improved particle swarm optimization*, *Optics Communications* **392**, 2017, pp. 153–161, DOI: [10.1016/j.optcom.2016.10.027](https://doi.org/10.1016/j.optcom.2016.10.027).
- [22] YANG J., ZHANG J., XU S., CHANG S., *Beam splitter based on Bragg grating-assisted coupler*, *Chinese Optics Letters* **13**(s1), 2015, p. S12501.
- [23] GAO Z.H., CHEN X.H., PENG D.L., *Online self-calibration system for time grating angular displacement sensor*, *Guangxue Jingmi Gongcheng/Optics and Precision Engineering* **23**(1), 2015, pp. 93–101, DOI: [10.3788/OPE.20152301.0093](https://doi.org/10.3788/OPE.20152301.0093).
- [24] SU Y., *Material Mechanics*, China: Renmin Educational Press, 1980, pp. 106–150.

*Received July 1, 2020
in revised form August 2, 2020*